International Journal of Recent Advances in Multidisciplinary Topics
Volume 6, Issue 10, October 2025
www.ijramt.com | E-ISSN: 2582-7839 | RESAIM Publishing (www.resaim.com)

Nonlinear Dynamic Analysis of Rotor-Bearing System with Coupled Fault of Parallel Misalignment, Unbalance and Impact Rubbing

In-Chol Kim[1], Jong-Hyang Choe[2], Kum-Song Ri[3*]
[1,2,3]Faculty of Mechanical Science and Technology, Kim Cheak University of Technology, Pyongyang, Democratic People's Republic of Korea

***Abstract*: Misalignment and rubbing faults between the rotor and stator of rotor-bearing system are the most common faults of rotating machines. In this paper, the nonlinear dynamic behavior of rotor-bearing system with coupled fault of parallel misalignment, unbalance and rubbing is investigated. The equations of motion of the rotor system are derived by Lagrange's equations, and many techniques such as bifurcation diagram, Poincare diagram, axial orbit, time domain waveform and amplitude spectrum diagram are employed to study the dynamic behavior of rotor system with rubbing, mass unbalance and parallel misalignment faults. The effect of variation of the parallel misalignment on various nonlinear phenomena such as periodic, three-periodic and quasi-periodic motions is investigated. Finally, some significant results for the safe operation and accurate identification of faults in rotating machinery are provided.**

***Keywords*: rotor-bearing system, parallel misalignment, impact rubbing, nonlinear dynamics, bifurcation.**

1. Introduction

With the rapid development of science and technology, many modern machines are being developed in the machine industry. The faults occurring in the modern machines are difficult to predict, the cause is very complex and the types of faults are very diverse. Misalignment, mass balance and rubbing fault of rotor-bearing system are the most common faults of rotating machinery. The smaller the clearance between the rotor and stator, the higher the efficiency of the rotating machine, but the possibility of impact rubbing fault due to the rotor misalignment is greatly increased. In the misaligned rotating machine, the motion of the rotor may cause mechanical vibration, eccentricity of the coupling, oil whirl and oil whip of bearing, impact rubbing between rotor and stator, etc., which are very dangerous for the stable operation of the system [1]. Therefore, it is very important to study the dynamic characteristics of rotor misalignment –impact rubbing coupled fault and improve its operational stability.

In the past, a series of studies on the dynamic behaviour of rotor-bearing systems with different faults have been carried out. The effect of misalignment faults and nonlinear oil-film forces on the system response of an unsymmetrical rotor-bearing system with parallel misalignment was analysed by Li [2]. Li et al. [3] carried out nonlinear dynamic analysis of rotor-bearing system with misaligned gear couplings. In their study, various frequency components of transversely misaligned rotor system and anomalous frequency components in torsional direction were found. Redmond [4] identified the influence of various factors such as angular misalignment, coupling stiffness and static preload caused by misalignment between the two rotors on the dynamic stability and vibration characteristics of two rigid rotors connected with misaligned flexible couplings. Their study has a very important significance in the field of nonlinear vibration of rotor-bearing systems. Simon [5] investigated the influence of parameters based on Monte Carlo simulations in large-scale turbines, where the coupling misalignment and mass unbalance were considered as undetermined vibrations.

Several studies have been carried out to discuss the nonlinear bearing viscous force analysis model and the effect of the oil film force on the response of the system. Ma et al. [6] studied the effect of the film instability of sleeve bearings on some nonlinear vibration mechanisms of a misaligned rotor system. A nonlinear oil film force analysis model of short journal bearing was proposed and the effect of oil film forces on the system response of a nonlinear system was investigated [7]-[9]. Ji [10] studied the complex dynamics of a simple rotor with one loose end bearing, and Chu [11] investigated the various types of cyclic motion, quasi-cycles and chaos of a system with varying rotational speed.

The study of rotor-bearing systems with various hybrid faults has been further performed, for example, the equations of motion of Jeffcott rotor with hybrid fault due to bearing loosening and impact rubbing were established and the effect of hybrid fault on rotor system stiffness was analysed by Muszynska [12]. The nonlinear dynamic equations of the hydro-turbine generator were established and the influence of some parameters such as generator rotational speed, rotor mass eccentricity, etc. on the radial vibration characteristics of the generator shaft system was analysed by Gustavsson [13]. Their study showed that the system response is mainly a simple periodic motion, but a quasi-periodic motion may occur in some parts. Ma et al. [14] proposed a coupled vibration model of the

*Corresponding author: kyj801031@star-co.net.kp

generator and building machine foundation, in which the bearing uncertainty and the interconnection of the plant building and the generator were taken into account. Wei [15] studied the nonlinear bearing dynamic characteristics and the influence of the flexibility of the plant building machine foundation on the dynamic characteristics of a hydro turbine-generator by using the finite element method.

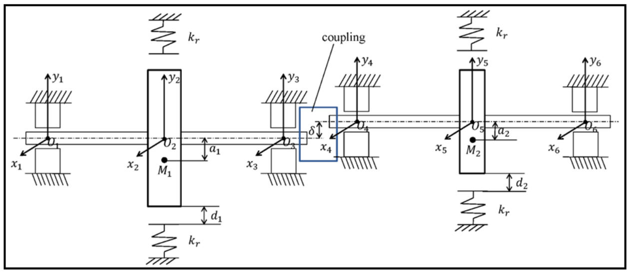

Fig. 1. Rotor-bearing system with coupled fault

Most of the above studies focus on the simple faults of rotor-bearing systems. However, the most frequent faults in rotor-bearing systems are due to mass unbalance or impact rubbing.

In this paper, a nonlinear dynamic model and differential equations of motion of rotating system with various vibration faults are proposed based on the theory and method of nonlinear rotor dynamics. In addition, many techniques such as bifurcation diagram, Poincare diagram, axial orbit, time domain waveform and amplitude spectrum diagram are employed to study the dynamic behavior of rotor system with rubbing, mass unbalance and parallel misalignment faults.

2. Dynamic Model

A. System Descriptions

Fig. 1 illustrates a rotor-bearing system with coupled fault of parallel misalignment, unbalance and impact rubbing, in which two rotors with parallel misalignment δ are rigidly connected to each other. It is assumed that each rotor is mounted in the center of a flexible shaft supported by a nonlinear oil film bearing and rotates in its own plane without the gyroscopic effect.

B. Mathematical Model

1) Impact Rubbing Force Model

Fig. 2 illustrates the impact rubbing force model of rotor 1, in which the elastic impact between rotor and stator is considered. O_3, O_2 and O_2' are the geometric center of bearing, the geometric center and the center of mass of rotor 1, respectively; Ω is the rotational speed; d_1 is the clearance between stator and rotor 1; a_1 is the mass eccentricity; r_1 denotes the radial displacement of the rotor shaft; φ_0 is the initial phase of mass unbalance.

According to the Coulomb friction law, the friction force is decomposed in the normal and tangential directions. Then, when the rotor 1 is impacted by stator, the normal collision force P_N and the tangential rubbing force P_T can be expressed as

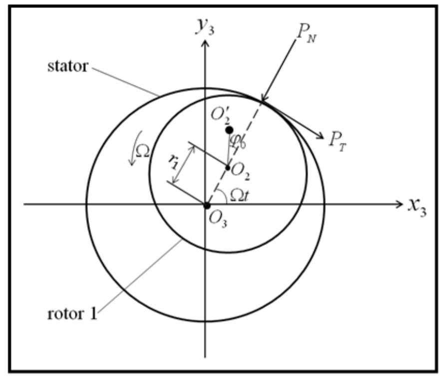

Fig. 2. Impact rubbing force model of rotor 1

$$\begin{cases} P_T = f \cdot P_N \\ P_N = (r_1 - d_1)K_r \qquad r_1 \geq d_1 \end{cases} \tag{1}$$

where Kr is the radial stiffness of the stator, and f is the rubbing coefficient between the rotor and the stator.

The component of the impact rubbing force along x and y directions as follows.

$$\begin{Bmatrix} P_x \\ P_y \end{Bmatrix} = \begin{bmatrix} -\cos\Omega t & \sin\Omega t \\ -\sin\Omega t & -\cos\Omega t \end{bmatrix} \begin{Bmatrix} P_N \\ P_T \end{Bmatrix} \tag{2}$$

where $\sin\Omega t = \dfrac{y_2}{r_1}, \quad \cos\Omega t = \dfrac{x_2}{r_1}$.

From Eqs. (1) and (2), the impact rubbing forces of rotor 1 along the x and y directions can be written as,

$$\begin{cases} P_{1x} = -K_r\,(1 - d_1/r_1)(x_2 - \mu \cdot y_2) \\ P_{1y} = -K_r\,(1 - d_1/r_1)(\mu \cdot x_2 + y_2) \end{cases} \quad r_1 \geq d_1 \tag{3}$$

Similarly, the impact rubbing forces of rotor 2 along the x and y directions are,

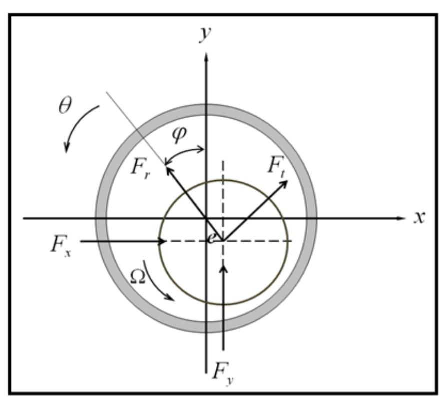
Fig. 3. Schematic diagram of oil film bearing

$$\begin{cases} P_{2x} = -K_r\,(1-d_2/r_2)(x_5-\mu\cdot y_5) \\ P_{2y} = -K_r\,(1-d_2/r_2)(\mu\cdot x_5+y_5) \end{cases} \quad r_2 \ge d_2 \tag{4}$$

where $r_1 = \sqrt{{x_2}^2+{y_2}^2}$, $r_2 = \sqrt{{x_5}^2+{y_5}^2}$.

2) The model of Nonlinear Oil Film Force

Fig. 3 illustrates a schematic diagram of oil film bearing. In order to study the dynamic characteristics of rotor bearing system, the nonlinear oil film force of bearing should be known. However, the calculation of nonlinear oil film forces is difficult without some assumptions such as infinitely long bearings or very short bearings [16].

Assuming a very short sliding bearing for the simplification of the problem, the Reynolds equation can be written as [17].

$$p(\theta,z) = -\frac{3\mu}{h^3}\left(\frac{L^2}{4}-z^2\right)\left[(\Omega-2\dot\varphi)\frac{\partial h}{\partial\theta}+2\dot e\cos\theta\right] \tag{5}$$

where $h = c + e\cos\theta = c(1+\varepsilon\cos\theta)$ is the thickness of oil film; e and φ are the equilibrium positions the rotor centerline; θ is the circumferential coordinate; μ is the visiocity; R is radius of bearing; L is length of bearing, c is the bearing clearance; ε is the bearing eccentricity.

If the relative pressure at the bearing tip is zero, the oil pressure can be expressed as,

$$\frac{\partial}{\partial z}\left(\frac{h^3}{\mu}\frac{\partial p}{\partial z}\right) = 6\left[(\Omega-2\dot\varphi)\frac{\partial h}{\partial\theta}+2\dot e\cos\theta\right] \tag{6}$$

Note that the boundary condition for the pressure could not be imposed in the circumferential direction. Therefore, the analytical method can only be used for journal bearings without shaft grooves by using Sommerfeld boundary conditions. Then, the radial and tangential oil film forces as follows.

$$\begin{aligned} F_{jr} &= -R\mu\frac{L^3}{c^2}\pi\dot\varepsilon_j\frac{\left(1+2{\varepsilon_j}^2\right)}{\left(1-{\varepsilon_j}^2\right)^{5/2}} \\ F_{jt} &= -R\mu\frac{L^3}{c^2}\pi\varepsilon_j\frac{\left(\Omega-2\dot\varphi_j\right)}{2\left(1-{\varepsilon_j}^2\right)^{3/2}} \end{aligned} \quad j\text{=1,3,4,6} \tag{7}$$

From Eq. (7), the oil film forces in Cartesian coordinate system are expressed as,

$$\begin{cases} F_{jx}(x_j,y_j,\dot x_j,\dot y_j) = -F_{jr}\sin\varphi_j + F_{jt}\cos\varphi_j \\ F_{jy}(x_j,y_j,\dot x_j,\dot y_j) = F_{jr}\cos\varphi_j + F_{jt}\sin\varphi_j \end{cases} \quad j\text{=1,3,4,6} \tag{8}$$

where $\cos\varphi_j = -\dfrac{y_j}{e_j}$, $\sin\varphi_j = -\dfrac{x_j}{e_j}$, $e_j = \sqrt{x_j^2+y_j^2}$,

$$\varepsilon_j = \frac{e_j}{c},\quad \frac{d\varphi_j}{dt} = \frac{\dot y_j x_j - \dot x_j y_j}{{e_j}^2},$$

$$\frac{de_j}{dt} = \frac{x_j\dot x_j + y_j\dot y_j}{e_j}.$$

3) Equations of Motion

The total kinetic energy of the system can be expressed as,

$$\begin{aligned} T =& \frac{1}{2}m[\dot x_1^2+\dot y_1^2+\dot x_3^2+\dot y_3^2+\dot x_4^2+\dot y_4^2+\dot x_6^2+\dot y_6^2] \\ &+\frac{1}{2}M_1[(\dot x_2-a_1\Omega\sin(\varphi_0+\Omega t))^2+(\dot y_2+a_1\Omega cos(\varphi_0+\Omega t))^2] \\ &+\frac{1}{2}M_2[(\dot x_5-a_2\Omega\sin(\varphi_0+\Omega t))^2+(\dot y_5+a_2\Omega cos(\varphi_0+\Omega t))^2] \\ &+\frac{1}{2}J_1\Omega^2+\frac{1}{2}J_2\Omega^2 \end{aligned} \tag{9}$$

where M_1, M_2 and m means the equivalent masses including the rotors and the shafts, respectively; a_1, a_2 are the eccentricity of rotors, respectively; Ω is the rotational speed.

When a collision between the stator and the rotor occurs, i.e. $r_1 \ge d_1$, $r_2 \ge d_2$, the potential energy can be expressed as,

$$\begin{aligned} U =& \frac{1}{2}k_1(x_1-x_2)^2+\frac{1}{2}k_1(y_1-y_2)^2+\frac{1}{2}k_1(x_2-x_3)^2 \\ &+\frac{1}{2}k_1(y_2-y_3)^2+\frac{1}{2}k_2(x_4-x_5)^2+\frac{1}{2}k_2(y_4-y_5)^2 \\ &+\frac{1}{2}k_2(x_5-x_6)^2+\frac{1}{2}k_2(y_5-y_6)^2+mg(y_1+y_3+y_4+y_6) \\ &+M_1g(y_2+a_1\cos(\varphi_0+\Omega t))+M_2g(y_5+a_2\cos(\varphi_0+\Omega t)) \\ &+\frac{1}{2}K_r(r_1-d_1)^2+\frac{1}{2}K_r(r_2-d_2)^2 \end{aligned} \tag{10}$$

Fig. 4 shows the motion relationship between two adjacent rotors with parallel misalignment, in which ϕ is the angle between the x-axis and the straight line connecting nodes 3 and 4.

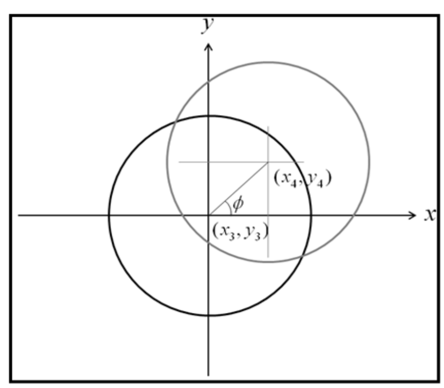

Fig. 4. The motion relationship between the adjacent rotors with the parallel misalignment

The displacements of two adjacent rotors are coupled because of the parallel misalignment between them, and thus the constraints are imposed on the rotor system based on the analytical dynamics theory.

Thus, the constraint function is defined as,

$$f(x_3, y_3, x_4 y_4) = (x_3 - x_4)^2 + (y_3 - y_4)^2 - \delta^2 = 0 \tag{11}$$

where δ means rotor misalignment.

The above constraint is holonomic and can be expressed in another form by introducing an angle variable as,

$$\begin{cases} x_3 - x_4 = \delta \cos\phi \\ y_3 - y_4 = \delta \sin\phi \end{cases} \tag{12}$$

By substituting the constraint Eq. (12) into Eqs. (9) and (10), the kinetic and potential energies can be written as,

$$\begin{aligned} T = {} & \frac{1}{2} m[\dot{x}_1^2 + \dot{y}_1^2 + (\dot{x}_4 - \delta\dot{\phi}\sin\phi)^2 + (\dot{y}_4 + \delta\dot{\phi}\cos\phi)^2 + \dot{x}_4^2 + \dot{y}_4^2 + \dot{x}_6^2 + \dot{y}_6^2] \\ & + \frac{1}{2} M_1 [(\dot{x}_2 - a_1 \Omega \sin(\varphi_0 + \Omega t))^2 + (\dot{y}_2 + a_1 \Omega cos(\varphi_0 + \Omega t))^2] \\ & + \frac{1}{2} M_2 [(\dot{x}_5 - a_2 \Omega \sin(\varphi_0 + \Omega t))^2 + (\dot{y}_5 + a_2 \Omega cos(\varphi_0 + \Omega t))^2] \\ & + \frac{1}{2} J_1 \Omega^2 + \frac{1}{2} J_2 \Omega^2 \end{aligned} \tag{13}$$

$$\begin{aligned} U = {} & \frac{1}{2} k_1 (x_1 - x_2)^2 + \frac{1}{2} k_1 (y_1 - y_2)^2 + \frac{1}{2} k_1 (x_2 - \delta\cos\phi - x_4)^2 \\ & + \frac{1}{2} k_1 (y_2 - \delta\sin\phi - y_4)^2 + \frac{1}{2} k_2 (x_4 - x_5)^2 + \frac{1}{2} k_2 (y_4 - y_5)^2 \\ & + \frac{1}{2} k_2 (x_5 - x_6)^2 + \frac{1}{2} k_2 (y_5 - y_6)^2 + mg(y_1 + y_4 + \delta\sin\phi + y_4 + y_6) \\ & + M_1 g (y_2 + a_1 \cos(\varphi_0 + \Omega t)) + M_2 g (y_5 + a_2 \cos(\varphi_0 + \Omega t)) \\ & + \frac{1}{2} K_r (r_1 - d_1)^2 + \frac{1}{2} K_r (r_2 - d_2)^2 \end{aligned} \tag{14}$$

Generally, the oil film forces $F_{ix}(x_i, y_i, \dot{x}_i, \dot{y}_i)$ and $F_{iy}(x_i, y_i, \dot{x}_i, \dot{y}_i)$ are related to the displacements of the rotors and their velocities. However, if the misalignment between two rotors exists, as shown in Fig. 1, the functions of the oil film forces in bearing 3 can be expressed as,

$$\begin{cases} F_{3x} = F_{3x}(x_4 + \delta\cos\phi, y_4 + \delta\sin\phi, \dot{x}_4 - \delta\sin\phi, \dot{y}_4 + \delta\dot{\phi}\cos\phi) \\ F_{3y} = F_{3y}(x_4 + \delta\cos\phi, y_4 + \delta\sin\phi, \dot{x}_4 - \delta\sin\phi, \dot{y}_4 + \delta\dot{\phi}\cos\phi) \end{cases} \tag{15}$$

The generalized force vector including nonlinear film forces on the journal bearings are expressed by,

$$Q = \{F_{ix}, F_{jy}\}^T \quad i = 1,3,4,6 \quad j = 1,3,4,6 \tag{16}$$

The generalized coordinate system is,

$$q = \{x_1, y_1, x_2, y_2, x_4, y_4, x_5, y_5, x_6, y_6, \phi\} \tag{17}$$

Based on Lagrange's equation,

$$\frac{d}{dt}\frac{\partial T}{\partial \dot{q}_i} - \frac{\partial T}{\partial q_i} + \frac{\partial U}{\partial q_i} = Q_i \tag{18}$$

where generalized force Q_i is

$$\begin{aligned} & Q_1 = F_{1x} && Q_7 = P_{2x} \\ & Q_2 = F_{1y} && Q_8 = P_{2y} \\ & Q_3 = P_{1x} && Q_9 = F_{6x} \\ & Q_4 = P_{1y} && Q_{10} = F_{6y} \\ & Q_5 = F_{3x} + F_{4x} && Q_{11} = 0 \\ & Q_6 = F_{3y} + F_{4y} && \end{aligned} \tag{19}$$

Then, the general equations of motion taking into account the effects of misalignment, mass unbalance and impact rubbing are expressed as follows,

$$\overline{\mathbf{M}}\ddot{q} + \overline{\mathbf{K}}q = \overline{\mathbf{F}} \tag{20}$$

Where

$$\overline{\mathbf{M}} = \begin{bmatrix} m & 0 & 0 & 0 & 0 & 0 & 0 & 0 & 0 & 0 & 0 \\ 0 & m & 0 & 0 & 0 & 0 & 0 & 0 & 0 & 0 & 0 \\ 0 & 0 & M_1 & 0 & 0 & 0 & 0 & 0 & 0 & 0 & 0 \\ m & 0 & 0 & M_1 & 0 & 0 & 0 & 0 & 0 & 0 & 0 \\ m & 0 & 0 & 0 & 2m & 0 & 0 & 0 & 0 & 0 & -m\delta\sin\phi \\ m & 0 & 0 & 0 & 0 & 2m & 0 & 0 & 0 & 0 & m\delta\cos\phi \\ m & 0 & 0 & 0 & 0 & 0 & M_2 & 0 & 0 & 0 & 0 \\ m & 0 & 0 & 0 & 0 & 0 & 0 & M_2 & 0 & 0 & 0 \\ m & 0 & 0 & 0 & 0 & 0 & 0 & 0 & m & 0 & 0 \\ m & 0 & 0 & 0 & 0 & 0 & 0 & 0 & 0 & m & 0 \\ 0 & 0 & 0 & 0 & -m\delta\sin\phi & m\delta\cos\phi & 0 & 0 & 0 & 0 & \delta^2 m \end{bmatrix}$$

$$\overline{\mathbf{K}} = \begin{bmatrix} k_1 & 0 & -k_1 & 0 & 0 & 0 & 0 & 0 & 0 & 0 & 0 \\ 0 & k_1 & 0 & -k_1 & 0 & 0 & 0 & 0 & 0 & 0 & 0 \\ -k_1 & 0 & 2k_1 + (1 - \frac{r_1}{d_1})K_r & 0 & -k_1 & 0 & 0 & 0 & 0 & 0 & 0 \\ 0 & -k_1 & 0 & 2k_1 + (1 - \frac{r_1}{d_1})K_r & 0 & -k_1 & 0 & 0 & 0 & 0 & 0 \\ 0 & 0 & -k_1 & 0 & k_1 + k_2 & 0 & -k_2 & 0 & 0 & 0 & 0 \\ 0 & 0 & 0 & -k_1 & 0 & k_1 + k_2 & 0 & -k_2 & 0 & 0 & 0 \\ 0 & 0 & 0 & 0 & -k_2 & 0 & 2k_2 + (1 - \frac{r_2}{d_2})K_r & 0 & -k_2 & 0 & 0 \\ 0 & 0 & 0 & 0 & 0 & -k_2 & 0 & 2k_2 + (1 - \frac{r_2}{d_2})K_r & 0 & -k_2 & 0 \\ 0 & 0 & 0 & 0 & 0 & 0 & -k_2 & 0 & k_2 & 0 & 0 \\ 0 & 0 & 0 & 0 & 0 & 0 & 0 & -k_2 & 0 & k_2 & 0 \\ 0 & 0 & k_1\delta\sin\phi & -k_1\delta\cos\phi & -k_1\delta\sin\phi & -k_1\delta\sin\phi & 0 & 0 & 0 & 0 & 0 \end{bmatrix}$$

$$\overline{\mathbf{F}} = \left\{ \begin{array}{c} F_{1x} \\ F_{1y} - mg \\ P_{1x} + k_1 \delta \cos\phi + M_1 a_1 \Omega^2 \cos(\varphi_0 + \Omega t) \\ P_{1y} + k_1 \delta \sin\varphi + M_1 a_1 \Omega^2 \sin(\varphi_0 + \Omega t) - M_1 g \\ F_{3x} + F_{4x} + m\delta\dot{\phi}^2 \cos\phi - k_1 \delta \cos\phi \\ F_{3y} + F_{4y} + m\delta\dot{\phi}^2 \sin\phi - k_1 \delta \sin\phi - 2mg \\ P_{2x} + M_2 a_2 \Omega^2 \cos(\varphi_0 + \Omega t) \\ P_{2y} + M_2 a_2 \Omega^2 \sin(\varphi_0 + \Omega t) - M_2 g \\ F_{6x} \\ F_{6y} - mg \\ - mg\delta \cos\phi \end{array} \right\}$$

3. Nonlinear Dynamic Analysis

A. Parameters of System

$M_1 = 2.5 \times 10^4 kg$, $M_2 = 10^5 kg$, $m = 1000 kg$, $a_1 = 0.5mm$, $a_2 = 0.4mm$, $k_1 = 1.0 \times 10^7 N/m$, $k_2 = 1.2 \times 10^7 N/m$, $K_r = 2.5 \times 10^8 N/m$, $d_1 = 1mm$, $d_2 = 1mm$, $f = 0.01$, $c = 0.2mm$, $\mu = 0.018 Pa \cdot s$, $R = 0.15m$, $\mathrm{L}/2R = 0.25$

B. Influence of Parallel Misalignment

For the convenience of calculation composition and analysis, the dimensionless transformations are introduced as,

$$X = \frac{x}{\delta},\ Y = \frac{y}{\delta},\ D = \frac{d}{\delta} \tag{21}$$

Fig. 5 shows the bifurcation diagrams of the generator rotor and turbine rotor with different parallel misalignments and mass eccentricities. The response of the rotor system contains periodic, three-periodic and quasi-periodic motions in the range of D=0–2.

Fig. 6 illustrates the Poincaré maps, axis orbits, time histories and amplitude spectrum on the response of the rotor system for different D.

When misalignment is small, the response of the rotor system is complicated with the effect of mass eccentricity. At D=0.08, there exist twenty-two isolated points in the Poincaré map and two discrete frequency components in the amplitude spectrum. The rotor center trajectory displays 22T periodic motion in the axis contrail. As parallel misalignment increasing, the motion reveals different phenomena. At D=0.5, two discrete frequency components in the frequency spectrum arise and there is a closed curve in the Poincaré map. The rotor center trajectory is irregular, and beat vibration is observed on the time history. All of these give proof of that the motion is quasi-periodic. The closed form of the attractor is decomposed in the Poincaré map at D=0.95 as shown in Fig. 6c.

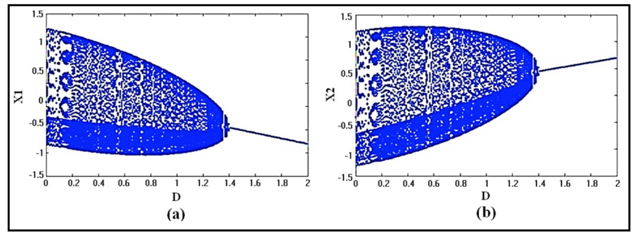

Fig. 5. Bifurcation diagrams of the generator rotor and turbine rotor response with parallel misalignment D as a control parameter (e_1 = 0.5 mm and e_2 = 0.4 mm)

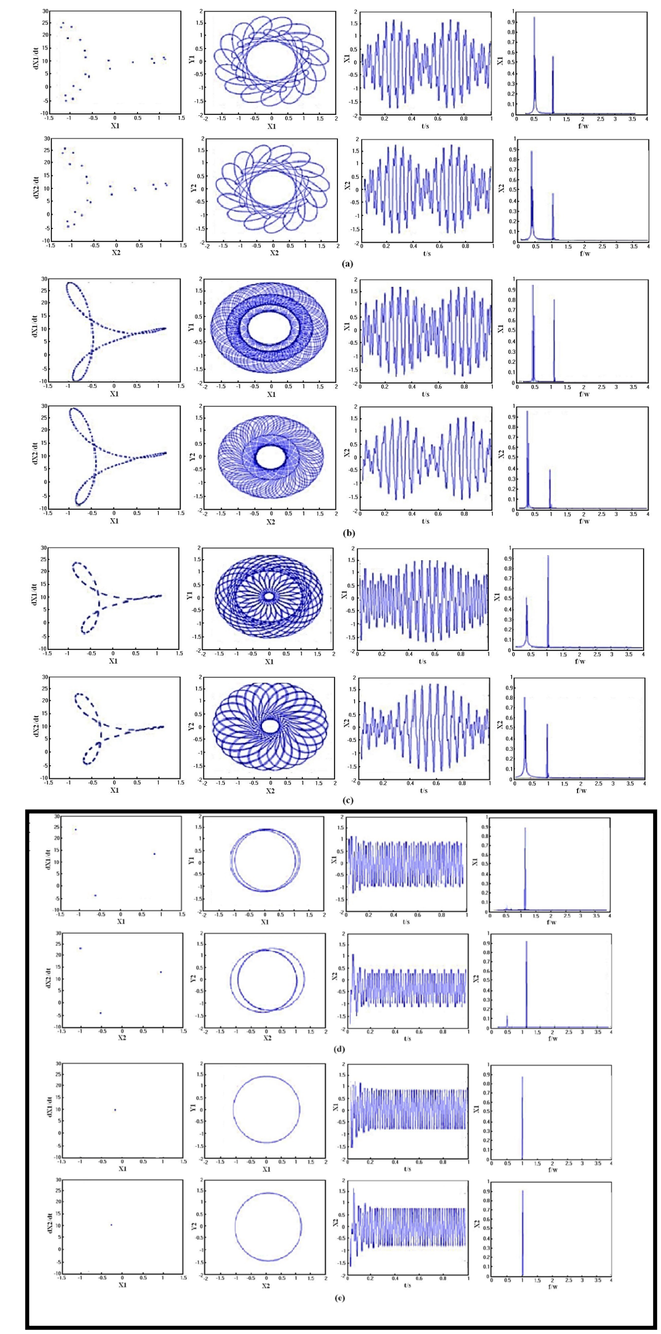

Fig. 6. Poincaré maps, axis orbits, times-histories and amplitude spectrums on the response of the generator rotor and turbine rotor at different parallel misalignment. a) D = 0.08, b) D = 0.5, c) D = 0.95, d) D = 1.4, e) D = 1.5

At D=1.4, the motion becomes a sub-synchronous vibration with period-three and its attractor is three isolated points, exhibiting three different circular rings in the axis contrail and different amplitudes in time history correspondingly. As D exceeds 1.4, the motion comes into period-one because the rotor system reaches dynamic balance. Fig. 6e illustrates the dynamic characteristics for D=1.5. There exists an isolated point in the Poincaré map, a limited circle in the rotor center trajectory and one discrete frequency component in the frequency spectrum, which represents period-one motion. Although the two rotors are rigidly coupled by the shafts, dynamic characteristics of the generator rotor with the impact rubbing force are more complex than those of the turbine rotor such as axis orbits and time histories.

From amplitude spectrums of Fig. 6a–d, we can observe some low frequencies with large amplitude at 0.3–0.4× components especially, besides 1× component. Amplitude of the generator rotor at 1× component is increasing constantly, but it is opposite for the turbine rotor with the increase in parallel misalignment. At the same time, the low frequency amplitude of both rotors is decreasing. The response of the sub-harmonic results forms a coupling fault with parallel axis misalignment, and the impact friction on the rotor system produces a larger amplitude of low frequency than that of the 1 × component. The phenomenon, as depicted in Fig. 6a–d, can be defined as a typical feature for the coupling faults, which would provide important theory basis for diagnosing the fault pattern.

C. Influence of Mass Eccentricity

Mass eccentricity of rotor is one of the primary factors affecting dynamic characteristics of the coupled system. The graphs shown in Fig. 7 exhibit different bifurcation diagrams of the system response, where D is the control parameters with different mass eccentricity of the two rotors. It obviously demonstrates that the influence of mass eccentricity surpasses radial vibration of the rotor system.

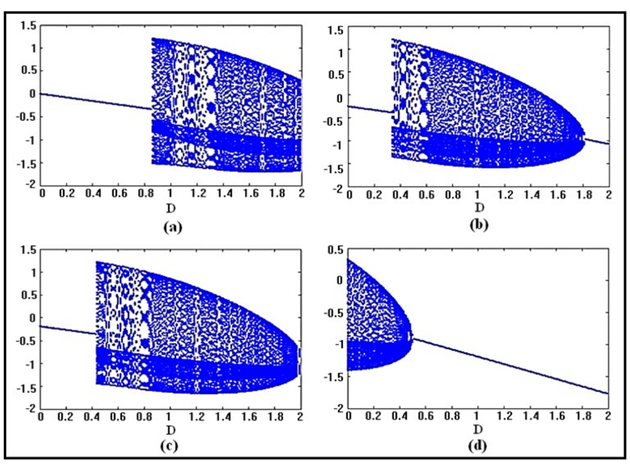

Fig. 7. Bifurcation diagrams of the rotor system with D as a control parameter for different e_1 and e_2. a) $e_1 = 0$, $e_2 = 0$, b) $e_1 = 0.5$mm, $e_2 = 0$, c) $e_1 = 0$, $e_2 = 0.5$ mm, d) $e_1 = 0.8$ mm, $e_2 = 0.8$ mm

In Figure 7a, the bifurcation diagram at $e_1 = e_2 = 0$ is plotted to show the process from the period-one motion to quasi-periodic motion. Comparing Fig. 7a and b, we can see that the instability misalignment of the latter is bigger than that of the former. In other words, the region of aperiodic responses is moved forward. The influence of the mass eccentricity distance of the generator rotor is more pronounced, as shown in in Fig. 7c. Figure 7 shows the bifurcation diagrams of the rotor system (e_1=0.5 mm, e_2 = 0.4 mm) and the transition from the quasi-periodic motion to one-periodic motion. Then, as shown in Fig. 7d (e_1 = 0.8 mm and e_2 = 0.8 mm), we can conclude that the more the mass eccentricity distance increases, the wider the quasi-periodic range of motion. Numerical simulation results show that as the mass eccentricity increases, impact rubbing occurs in advance and partial friction of the rotor is converted into full friction; finally, the response of the rotor system transits from quasi-periodic motion to synchronous motion with one-periodic.

4. Conclusion

In this paper, a model of a rotor-bearing system with parallel misalignment, impact rubbing and mass imbalance faults is investigated to study the fault problem of the local friction of the generator rotor caused by the parallel misalignment and mass eccentricity. Some nonlinear analysis methods including bifurcation diagrams, Poincaré maps, axis orbits, time histories and amplitude spectrum diagrams are used to investigate the dynamic behavior of the discussed system. The conclusions obtained from the study are as follows:

1) The response of the rotor system contains periodic, three-periodic and complicated quasi-periodic motions in the range D =0~2. There are some low frequencies with large amplitude in the 0.3~0.4× components with large amplitude. Although the two rotors are coupled rigidly, dynamic characteristics of two rotors are slightly different.
2) The effect of mass eccentricity distance on the radial vibration of the rotor system is significant. As the mass eccentricity increases, the aperiodic response region of the rotor system moves continuously. Computational results show that the decrease of mass eccentricity and the increase of stiffness increase the stable-state region of the system and may prevent the occurrence of the abnormal vibration.

A. Acknowledgement

The work was carried out in Faculty of Mechanical Science and Technology of Kim Chaek University of Technology. The author would like to thank Mechanics Institute of the Faculty for their assistance in experimental part of the study. The author is thankful to the Head of the Department, Professor Hukjin Song for his help and encouragement.

B. Conflict of Interests

The author declares no conflict of interest.

C. Disclosure Statement

No potential conflict of interest was reported by the authors.

D. Data Availability

The data that support the findings of this study are available within the article.

References

[1] John Vance, Fouad Zeidan, Brian Murphy, 2010. Machinery vibration and rotor dynamics, 36, 1-419.

[2] Zigang Li., Jing Li., Ming Li., 2018. Analysis of the coupled lateral torsional vibration of a rotor-bearing system with a misaligned gear coupling, *Advances in Mechanical Engineering*, 10(5), 1-17.

[3] Li M., Yu L., 2001. Analysis of the coupled lateral torsional vibration of a rotor-bearing system with a misaligned gear coupling, *J Sound Vib*, 243, 283-300.

[4] Redmond I., 2010. Study of a misaligned flexibly coupled shaft system having nonlinear bearings and cyclic coupling stiffness - theoretical model and analysis, *J Sound Vib*., 329, 700-720.

[5] Simon G., 1992. Prediction of vibration behavior of large turbo machinery on elastic foundation due to unbalance and coupling misalignment, *Proc IMechE, Part C: J Mechanical Engineering Science*, 206, 29-39.

[6] Ma H, Wang XL, Niu HQ, et al., 2015. Oil-film instability simulation in an overhung rotor system with flexible coupling misalignment. *Arch Appl Mech*., 85, 893–907.

[7] Slim Bouaziz, Molka Attia Hili, et al., 2009. Dynamic behavior of hydrodynamic journal bearings in presence of rotor spatial angular misalignment, *Mechanism and Machine Theory,* 44, 1548-1559.

[8] G. Adiletta, A.R. Guido, C. Rossi., 1996. Chaotic motions of a rigid in short journal bearings. *Nonlinear Dynamics*, 10, 251-269.

[9] Jiun-Shen Wang, Cheng-Chi Wang., 2005, Nonlinear dynamic and bifurcation analysis of short aerodynamic journal bearings. *Tribology International*, 38, 740-748.

[10] Z. Ji, J.W. Zu., 1998. Method of multiple scales for vibration analysis of rotor-shaft system with non-linear bearing pedestal model., *Journal of Sound and Vibration*, 218(2), 293-305.

[11] F.L. Chu, Y. Tang., 2001. Stability and non-linear responses of a rotor-bearing system with pedestal looseness., *Journal of Sound and Vibration*, 241(5), 879-893.

[12] Muszyn´ska A., P. Goldman., 1995. Chaotic response of unbalanced rotor bearing stator systems with looseness or rubs. *Chaos, Solitons and Fractals*, 5(9), 1683-1704.

[13] R.K. Gustavsson., 2009. Evaluation of impact dynamics and contact forces in a hydropower rotor due to variations in damping and lateral fluid forces, *International Journal of Mechanical Sciences*, 51, 653-661.

[14] Z.Y. Ma, Z.Q. Song., 2009. Nonlinear dynamic characteristic analysis of the shaft system in water turbine generator set., *Chinese Journal of Mechanical Engineering*, 22(1), 124-131.

[15] S.H. Wei, L.J. Zhang., 2010. Vibration analysis of hydropower house based on fluid-structure coupling numerical method. Water Science and Engineering, 3(1), 75-84.

[16] Amamou A and Chouchane M. 2014. Nonlinear stability analysis of long hydrodynamic journal bearings using numerical continuation. *Mech Mach Theory,* 72, 17–24.

[17] J. Frene, D. Nicolas, B. degueurece, et al., 1990. Hydrodynamic Lubrication (Bearings and Thrust Bearings), *Elsevier science B.V.*, 33, 1-499. http://mtnet.dias.ie/data/download_data.html).